JOURNAL OF CATALYSIS **177,** 352–362 (1998)
ARTICLE NO. CA982112

Catalytic Reduction of Nitric Oxide by Methane in the Presence of Oxygen on Palladium-Exchanged Mordenite Zeolites

Claude Descorme,* Patrick Gélin,*,[1] Christine Lécuyer,† and Michel Primet*

*Laboratoire d'Application de la Chimie à l'Environnement, UMR CNRS 5634, Université Claude Bernard Lyon I, 43, Boulevard du 11 Novembre 1918, 69622 Villeurbanne Cedex, France; and †GAZ DE FRANCE, Direction de la Recherche, CERSTA, 361, avenue du Président Wilson, P.O. Box 33, 93211 La Plaine St-Denis Cedex, France

Received January 26, 1998; revised April 15, 1998; accepted April 18, 1998

Pd was introduced by exchange in non-dealuminated and dealuminated mordenites. After activation under oxygen at 500°C, NO adsorption revealed the presence of isolated Pd^{2+} ions and Pd/PdO particles. Two types of Pd ions were shown: the first one would be located in the small cavities and leads to the formation of dinitrosyl complexes, whereas the second one, probably sitting in the main channels, is responsible for the obtainment of mononitrosyl complexes. Pd/PdO particles are active in the direct combustion of CH_4 by oxygen and poorly active in the selective reduction (SCR) of NO. Pd ions are active for the NO SCR; the ions in the main channels are thought to be more active than the ions in the small cavities for accessibility reasons. In the case of the non-dealuminated mordenite catalyst, an activation under reactants is observed. Moreover, the activity is increased by the addition of 10 vol% water which is the opposite of the classical behavior of metal-loaded zeolites. Both phenomena are attributed to a migration of Pd ions from hidden to accessible sites. For the dealuminated sample, the observed deactivation seems to be due to a migration of isolated Pd ions into PdO particles located outside the zeolite matrix.

Key Words: **SCR; palladium; mordenite; dealumination; nitric oxide; methane.**

INTRODUCTION

In view of environmental/pollution prevention, compressed natural gas (CNG) appears to be an attractive alternative fuel for vehicles. Besides for economical reasons, CNG shows decided environmental advantages over gasoline or diesel: (i) CO_2 emissions are reduced due to the high H/C ratio of CH_4, which is the main component (85–95%) of natural gas; (ii) despite the absence of CNG-dedicated engines, the pollutants like CO, NO_x, and unburned hydrocarbons (UHC) emitted by CNG-fueled vehicles are strongly reduced, compared to noncatalyzed gasoline vehicles. However, in order to meet the more and more stringent regulations for the control of vehicle emissions, the CNG-fueled vehicles need to be equipped with catalytic converters able to remove the remaining CO, NO_x, and unburned methane from the exhaust gases. The catalytic reduction of NO_x by hydrocarbons has been studied extensively in the past few years, appearing as a promising process for the removal of dilute amounts of NO_x from exhaust gases in the presence of quite large amounts of oxygen (1–3). However, due to its particularly high stability, methane is very difficult to activate and most catalysts, when active, tend to burn methane by O_2 without removing NO_x. Therefore, the emission control of CNG-fueled vehicles requires the development of specific catalysts. Since the pioneering work by Li and Armor on Co^{2+}-exchanged ZSM-5 catalysts (4), new classes of transition metal-exchanged zeolite catalysts have been shown to selectively reduce NO_x by CH_4 in excess oxygen (5–17). Nontransition metal (Ga, In) loaded zeolites were also found to be very active for the reaction between CH_4 and NO_x (18–23). However, the activity of the latter catalysts is strongly decreased by the presence of water. On the contrary, Pd exchanged H-ZSM-5 and MOR catalysts (24–30), as well as, to a lesser extent, Co-H-ZSM-5 catalysts (7), appear much less sensitive to water, which makes them more attractive for being used in catalytic converters. For automotive applications, another problem is raised by the large range of temperatures (300–750°C) which the catalyst is submitted to, depending on the traffic conditions. The resistance of the catalyst toward severe steaming conditions is essential in view of its commercial application. It is well known that zeolites are sensitive to steaming, which induces the dealumination of the framework and, depending on the structure and the Si/Al ratio, the possible collapse of the structure. The catalytic properties of Pd-H-ZSM-5 catalysts of varying Si/Al ratios have been previously studied (31). In this paper, we were interested in the catalytic properties of Pd-exchanged mordenite catalysts in the selective reduction of nitric oxide by methane in the presence of oxygen. The influence of the Si/Al ratio on the catalytic activity and selectivity in this reaction was examined. The adsorption of NO on the Pd-H-MOR catalysts with varying Si/Al ratios was carefully investigated by FT-IR spectroscopy in order to

[1] Corresponding author. E-mail: Patrick.Gelin@univ-lyon1.fr.

0021-9517/98 $25.00

characterize the Pd sites. A stoichiometric interconversion between mono- and di-nitrosyl Pd complexes was shown. The localization of these complexes in the mordenite pores and their reactivity in the reduction of NO is discussed in the light of catalytic activity results.

EXPERIMENTAL

1. Sample Preparation

The starting mordenite sample obtained in the Na^+ form from Zeocat (ZM-060, Si/Al = 5.5) was first converted to the NH_4^+ form by exchanging with NH_4Cl. The resulting material contained 0.1 wt% Na (dry basis) and its chemical formula determined from elemental analysis was $Na_{0.13}(NH_4)_{7.76}\ Al_{7.89}\ Si_{40.11}\ O_{48}$ (Si/Al = 5.1). It is designated as NH_4-MOR. The NH_4-MOR sample was subsequently dealuminated according to the following procedure. 20 g of NH_4-MOR were deposited onto the frittered disk of a quartz reactor (40 mm ID, bed thickness = 8 mm) and heated from room temperature up 500°C under a 10 l/h oxygen stream at a heating rate of 0.5°C/min. After one hour calcination at 500°C, the reactor was purged for one hour with nitrogen flow (flow rate = 10 l/h) at the same temperature before increasing the temperature up to 650°C (heating rate of 5°C/min); 5 vol% water vapor was then added to the nitrogen stream for one hour at 650°C. An additional one hour purge under nitrogen at 650°C was carried out before decreasing the temperature down to room temperature. The sample was subsequently acid-leached by a 3 *M* HCl aqueous solution at 80°C for one hour under stirring, centrifuged, and thoroughly washed by distilled water. The complete sequence of thermal treatments followed by acid leaching was repeated three times and the resulting dealuminated mordenite sample was finally dried in air at 120°C overnight and designated as H-MOR-D. The H-MOR-D sample contained significant amounts of extraframework Al (EFAL) species (see Table 1). It has been shown that part of the extraframework Al species formed upon dealumination of mordenite by steaming–acid leaching cycles may be removed after a final washing by a $(NH_4)_2SiF_6$ solution (32). A suspension of 3 g of the H-MOR-D sample in 30 cm^3 of a buffered ammonium acetate solution (1.28 *M*) was stirred at 80°C while adding 10.5 cm^3 of a $(NH_4)_2SiF_6$ solution (0.367 *M*) at an injection rate of 0.745 cm^3/min. Stirring of the suspension at 80°C was maintained for one hour after the complete injection of the $(NH_4)_2SiF_6$ solution. After being thoroughly washed by distilled water until complete elimination of F^-ions, the resulting sample was dried in air at 120°C overnight and designated as H-MOR-D-W.

Pd was introduced by conventional exchange of the starting materials (NH_4-MOR and H-MOR-D-W) using aqueous solutions of tetrammine Pd(II) nitrate at 80°C for 24 h. The amount of Pd(II) salt was adjusted so as to obtain a theoretical value of 1 wt% Pd. After exchange, the preparation was thoroughly washed with deionized water, filtered, and dried at 120°C overnight. In order to decompose ammonium ions (if present) into protons and remove the ammine ligands from Pd complexes, the Pd-exchanged zeolite samples were subsequently activated under flowing oxygen from 25 to 500°C with a linear ramp rate of 0.5°C/min. The resulting samples were designated as Pd-H-MOR and Pd-H-MOR-D-W. The results of atomic absorption analysis are reported in Table 1. The expected level of Pd exchange of the H-MOR and H-MOR-D-W samples (corresponding to 1 wt% Pd) was reached.

2. Catalytic Activity Measurements

The experimental details for activity measurements were described elsewhere (26, 31). Briefly, the conversions of NO_x and CH_4 were measured using a U-shaped quartz reactor (16-mm ID) operating in a steady-state plug flow mode. Typically, 200 mg of catalyst were activated *in-situ* in oxygen flow at 500°C (linear ramp rate of 0.5°C/min) purged for one hour at 500°C by flowing helium and cooled to 250°C

TABLE 1

Main Physicochemical Characteristics of Fresh and Aged Pd Exchanged Mordenite Samples

Samples	Elemental analysis				^{27}Al NMR		XRD	N_2 ads.	
	Si/Al	Al/uc	Pd/uc	Pd (wt%)	FAL/uc[b]	EFAL/uc	% crystall.[d]	V_μ (cm^3/g)	% crystall.
H-MOR	5.1[a]	7.9[a]			6.1[c]	1.8	100	0.22	100
H-MOR-D	7.5	5.6			2.7	2.9	81	0.18	82
H-MOR-D-W	9.9	4.5			2.4	2.1	88	0.19	86
Pd-H-MOR	6.3	6.6	0.27	0.98	5.9	0.7	n.m.	0.20	91
Pd-H-MOR-D-W	11.9	3.7	0.25	0.92	2.4	1.3	n.m.	n.m.	n.m.

Note. n.m. = not measured.

[a] NH_4^+ form.

[b] By measuring the intensity of the 4-coordinate Al signal; reference = H-MOR (6.1 FAL/uc).

[c] Equal to the elemental composition corrected for the 6-coordinate Al contribution.

[d] Reference = H-MOR (%C = 100).

before contact with the reactants. The reaction mixture was adjusted so as to examine the catalytic activity under stoichiometric or lean conditions. It consisted of 2000 vpm NO, 1000 vpm CH_4, 1000 vpm O_2 (stoichiometry) or 6240 vpm O_2 (lean conditions) and helium as balance, at a total flow rate of 167 cm^3/min; vpm stands for ppm (v/v). (The apparent gas hourly space velocity (GHSV) was 30000 h^{-1}, based on the apparent bulk density of the zeolites, ca 0.5 g/cm^3.) Under lean conditions, the S ratio, defined as [oxidants]/[reductants] = $([O_2]+0.5[NO])/2[CH_4]$ equaled 3.62. Two cycles were successively operated, consisting of increasing the temperature from 250 up to 500°C (linear rate of 1°C/min), maintaining 500°C for 10 h, and decreasing the temperature to 250°C. For all samples, the catalytic activity of the activated sample was first examined under stoichiometric conditions before switching to the lean conditions.

The effluent gases were analyzed using two gas chromatographs equipped with TCD and FID detectors and NO_x infrared analyzers. Carbon and nitrogen balances were checked. The NO_x conversion was determined according to the equation

$$NO_x \text{ conversion } \% = ([NO]_0 + [NO_2]_0 - [NO] - [NO_2]) * 100/([NO]_0 + [NO_2]_0),$$

where $[NO]_0$ and $[NO_2]_0$ are the inlet concentrations of NO and NO_2, respectively, and [NO] and $[NO_2]$ are the outlet concentrations. The NO_2 formation was low in the whole range of temperature ($[NO_2] \leq 40$ vpm), almost independent of the temperature and ascribed to the NO oxidation in the dead volume of the apparatus. The CH_4 conversion was determined from the formation of CO_2; carbon monoxide was never observed.

Over Co-ZSM-5 catalysts, two reactions, NO reduction by CH_4 [1] and CH_4 combustion [2], have been suggested to occur (4–7):

$$CH_4 + 2\,NO + O_2 \rightarrow CO_2 + N_2 + 2\,H_2O \quad [1]$$

$$CH_4 + 2\,O_2 \rightarrow CO_2 + 2\,H_2O. \quad [2]$$

Reaction [1] was based upon the fact that the catalyst was not active for NO reduction in the absence of O_2 (4–8) below 500°C. The same was observed on Pd catalysts (24, 33). Accordingly, the selectivity towards NO reduction, S_{SCR}, defined as the fraction of methane involved in reaction [1], can be written

$$S_{SCR} = 0.5[NO]_0 C_{NO}/[CH_4]_0 C_{CH_4},$$

where C_{NO} and C_{CH_4} are the conversions of NO and CH_4, $[NO]_0$ is the inlet concentration of NO, and $[CH_4]_0$ is the inlet concentration of CH_4. In our experimental conditions, $0.5[NO]_0 = [CH_4]_0$, and $S_{SCR} = C_{NO}/C_{CH_4}$.

3. *Physicochemical Characterizations*

X-ray diffraction measurements were performed using CuKα radiation. Nitrogen adsorption–desorption isotherms were measured at −196°C with a homemade apparatus. The microporous volume was determined using the t-plot method. TEM micrographs were obtained by direct observation of the steamed samples by using a JEOL 100 CX microscope. The ^{27}Al MAS NMR spectra were obtained using a BRUKER MSL-300 spectrometer operating at 78.2 MHz.

The IR studies of NO or NO_2 adsorption were performed using self-supported samples wafers (18 mm diameter, weight of 30 mg) introduced into a homemade IR-cell allowing *in situ* studies at varying temperatures under controlled atmosphere (34). The samples were pretreated *in situ* in flowing oxygen at 500°C for 30 min (after a linear ramp rate of 10°C/min from 25 to 500°C). The cell was subsequently connected to a UHV system allowing a base pressure as low as 10^{-8} Torr (1 Torr = 101,325/760 Pa and the sample evacuated at 500°C for 3 h before being cooled down to 25°C and contacted with NO in the 0.02–0.4 Torr pressure range. The IR spectra were recorded at a resolution of 4 cm^{-1} on a Fourier-transform IR spectrometer Nicolet Magna 550. All the reported spectra have been corrected for the baseline (spectrum of the sample activated *in situ* and evacuated under vacuum at 25°C) in order to highlight the spectral changes resulting from the NO_x adsorption.

RESULTS

1. *Aluminum Composition and Crystallinity of Pd Exchanged Mordenite Catalysts*

The Al composition of the starting and dealuminated mordenite samples from elemental analysis is given in Table 1 and compared to the framework Al (FAL) composition calculated from ^{27}Al MAS NMR spectra.

The ^{27}Al MAS NMR spectrum of the NH_4-MOR sample exhibits only one intense line at ca 53 ppm from $Al(H_2O)_6^{3+}$ due to 4-coordinate (framework) Al (35), which suggests the absence of extraframework Al species. It is deduced that the framework Al composition of the NH_4-MOR sample is equal to the elemental Al composition; i.e. 7.9 Al per unit cell (Al/u.c.). Upon calcination, the intensity of the 4-coordinate Al line decreases while a line at ca 0 ppm from $Al(H_2O)_6^{3+}$ ascribed to 6-coordinate (extraframework) Al appears (35), indicating the removal of some structural Al ions upon calcination. Accordingly, the FAL composition of the H-MOR sample determined from the integrated intensity of the 4-coordinate Al line was found equal to 6.1 Al/u.c. Upon exchange with Pd, the FAL composition remained unchanged and most of EFAL species present in the H-MOR sample were removed as shown by the fairly good agreement between NMR and chemical analysis results reported in Table 1.

Repeated cycles of steaming and HCl leaching induced a decrease of the elemental Al composition down to 5.6 Al/u.c. The FAL composition from ^{27}Al MAS NMR decreased more severely upon these treatments, indicating that a large fraction of Al (2.9 Al/u.c.) was still deposited in the zeolite pores. This result was corroborated by the appearance of a broad line at ca 0 ppm. The final washing with $(NH_4)_2SiF_6$, while not affecting the FAL composition, removed 55% of the EFAL species produced upon the dealuminating treatment. Further exchange with Pd did not influence the framework Al content. The Pd-H-MOR-D-W sample still contained some EFAL species (1.3 Al/u.c.) as revealed by ^{27}Al MAS NMR.

The crystallinity of the mordenite samples was measured from XRD measurements and determination of microporous volumes using nitrogen adsorption–desorption isotherms at 77 K. The results, reported in Table 1, have shown a good agreement between both techniques. Dealumination by steaming–HCl cycles induced 18% loss of crystallinity. Final leaching with $(NH_4)_2SiF_6$ was accompanied by a small increase of crystallinity, fairly consistent with the partial removal of amorphous EFAL species.

2. *Catalytic Activity of Pd-MOR Catalysts*

2.1. Pd-H-MOR sample. The conversions of methane into CO_2 and nitric oxide into nitrogen over Pd-H-MOR are reported as a function of temperature in Figs. 1A and 1B. The selectivity in the nitric oxide reduction (S_{SCR}) defined as the fraction of methane involved in the SCR of NO by CH_4 (reaction 1) is plotted in Fig. 1C. From the experiment performed under stoichiometric conditions, i.e. immediately after activation in O_2 at 500°C, conversions of NO and CH_4 are observed to increase continuously with the reaction temperature without the formation of nitrous oxide. Conversely, the SCR selectivity smoothly decreases upon temperature increase, indicating that higher temperatures favor the combustion of methane by O_2. The same trend was reported on Pd-H-ZSM-5 catalysts containing more than ca 0.5 wt% Pd (36). It is noteworthy that conversions of methane and nitric oxide increase significantly with time on stream at 500°C and the conversions measured upon decreasing temperature are higher than those measured during the heating ramp. This conversion increase is accompanied by an increase of the selectivity for SCR. A small amount of nitrous oxide (representing a NO conversion less than 2%) is detected in the 400–300°C range. These results suggest modifications of the catalyst under reactants favoring the formation of sites responsible for the nitric oxide reduction.

The influence of oxygen concentration on the nitric oxide reduction is examined by switching to the lean feed immediately after the test in stoichiometric conditions and running the same temperature program. Upon temperature increase, conversions of CH_4 and NO (into N_2) are much higher than those measured in stoichiometric conditions. However, according to the selectivity plot, the combustion of methane by O_2 is slightly favored under lean conditions, compared to stoichiometric ones, and some N_2O forms (NO conversion into N_2O less than 3%) between 300 and 450°C. As observed with the stoichiometric mixture, the combustion of methane by O_2 is favored at higher temperatures. Maintaining the temperature for 10 h does not affect the NO conversion while the methane conversion decreases. As a result the selectivity for SCR slightly improves. Upon decreasing the reaction temperature, the NO conversion curve exactly superimposes the one obtained upon temperature rise, while the methane conversion diminishes more slowly with temperature. Again N_2O forms between 450 and 300°C (less than 5% NO conversion).

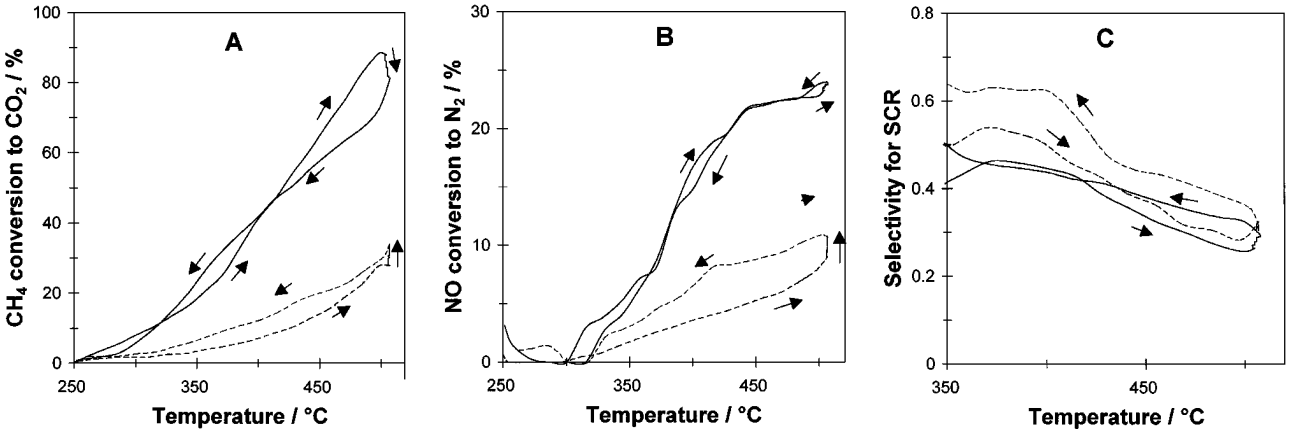

FIG. 1. Reaction of CH_4, NO, and O_2 over Pd-H-MOR catalyst as a function of the temperature: A, CH_4 to CO_2 conversion; B, NO to N_2 conversion; C, SCR selectivity for NO reduction as defined in the text. Full lines: lean mixture (2000 vpm NO, 1000 vpm CH_4, 6240 vpm O_2 in He). Broken lines: stoichiometric mixture (2000 vpm NO, 1000 vpm CH_4, 1000 vpm O_2 in He). GHSV: 30,000 h^{-1}.

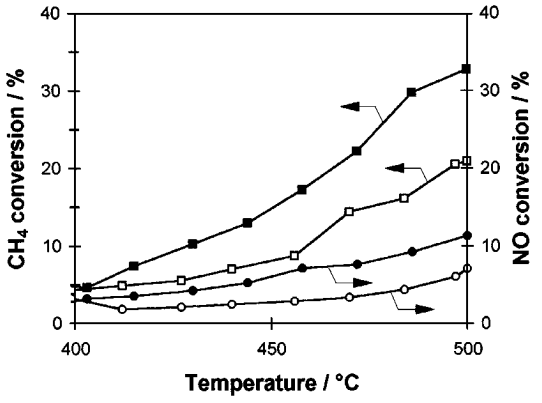

FIG. 2. Influence of water addition on CH_4 and NO conversions over Pd-H-MOR catalyst as a function of temperature for stoichiometric mixture. Open symbols: dry reactants; full symbols: wet reactants (10 vol% water). 2000 vpm NO, 1000 vpm CH_4, 1000 vpm O_2 in He, GHSV: 30,000 h^{-1}.

To evaluate the effect of water vapor on the reduction of NO by methane over Pd-H-MOR, 10 vol% water vapor was added to the stoichiometric feed and the conversions of NO and CH_4 measured between 250 and 500°C. The results are compared to those obtained in the absence of water in Fig. 2. The selectivity plots are reported in Fig. 3. Surprisingly, both conversions are enhanced when water is added to the feed. Moreover, as shown in Fig. 3, the catalytic activity of Pd-H-MOR in reduction of nitric oxide is significantly favored by the presence of water. This behavior strongly contrasts with that of a Pd-H-ZSM-5 catalyst (0.5 wt% Pd), for which adding 10 vol% water vapor to the feed markedly inhibits the reduction of NO (Fig. 3) by methane (25, 33).

2.2. Pd-H-MOR-D-W sample. Figures 4A and 4B show the conversions of CH_4 into CO_2 and NO into N_2 as a function of temperature over Pd-H-MOR-D-W under stoichiometric and lean conditions. In stoichiometric conditions, the conversion of CH_4 increases up to a maximum (63%) at 500°C, corresponding to the total consumption of O_2. The conversion of NO into N_2 shows a volcano curve, the maximum conversion of 25% being reached at 460°C. Beyond this temperature, traces of N_2O are detected. The selectivity for NO reduction (Fig. 4C) exhibits a continuous decrease with reaction temperature, indicating that combustion is more and more favored. At 500°C, the conversion of NO into N_2O increases from 2 to 8% with time on stream, while the formation of N_2 is stable. Upon decreasing the temperature, the formations of N_2, N_2O, and CO_2 decrease.

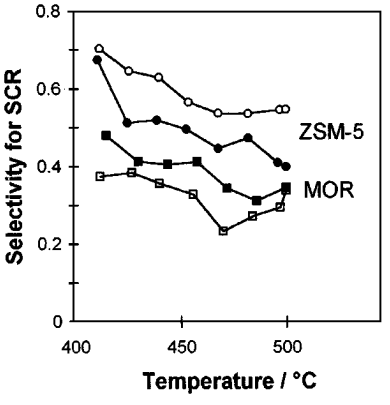

FIG. 3. Influence of water addition on the SCR selectivity in NO reduction over Pd-H-MOR (■, ❑) and Pd-H-ZSM-5 (●, ❍) catalysts; open symbols: dry reactants; full symbols: wet reactants (10 vol% water). 2000 vpm NO, 1000 vpm CH_4, 1000 vpm O_2 in He, GHSV: 30,000 h^{-1}.

On changing for lean conditions, the combustion is favored (Fig. 4C) and the SCR selectivity almost constant in the whole interval of temperatures. N_2O forms from 350°C up to 500°C (7% NO conversion on average) and its concentration is strongly increased, compared to stoichiometric conditions. The conversion curves obtained upon cooling show the same trend as upon temperature rise, with slightly lower conversion values. This indicates that the catalyst has not been significantly modified with time on stream at 500°C.

3. Transmission Electron Microscopy

In both Pd-H-MOR and Pd-H-MOR-D-W samples, large Pd (or PdO) particles can be observed on the outer surface of mordenite crystallites. In Pd-H-MOR, their size is about 1–2 nm while bigger and fewer particles (5–30 nm) are observed in Pd-H-MOR-D-W.

4. IR Study of NO Adsorption

4.1. Adsorption on Pd-H-MOR. Figure 5 shows the IR spectra of 0.4 Torr NO adsorption at 30°C on Pd-H-MOR activated in O_2 and evacuated at 500°C. Three bands form at 1906, 1875, and 1840 cm^{-1}, together with a broad asymmetric band at 2236 cm^{-1} of smaller intensity. The same band at 2236 cm^{-1} forms upon adsorption of NO_2 onto H-Mordenite at room temperature. Its formation parallels that of the 2136 cm^{-1} band upon adsorption of NO on Pd-H-ZSM-5 catalysts (27, 34, 36). It is therefore suggested to relate the 2236 cm^{-1} band to adsorbed NO_2 in interaction with mordenite protons. The bands at 1906, 1875, and 1840 cm^{-1} do not form when adsorbing NO on the H-MOR support. Evacuating the Pd-H-MOR sample under vacuum at room temperature does not affect the spectrum. It is concluded that the bands at 1906, 1875, and 1840 cm^{-1} are related to NO irreversibly bonded to Pd sites. Curve fitting of the spectrum shown in Fig. 5 was performed assuming gaussian peaks. Four distinct bands are necessary to obtain a satisfactory curve fitting. The band at 1878 cm^{-1} (type A, HWHM = 19 cm^{-1}) was already observed upon NO adsorption on Pd-H-ZSM-5 catalyst (27, 34, 36). This band is attributed to the NO stretching vibration of Pd mononitrosyl complexes anchored to the zeolite framework. The bands at 1908 and 1839 cm^{-1} (types B1 and B2, HWHM = 7.5 and 8.5 cm^{-1}, respectively) are

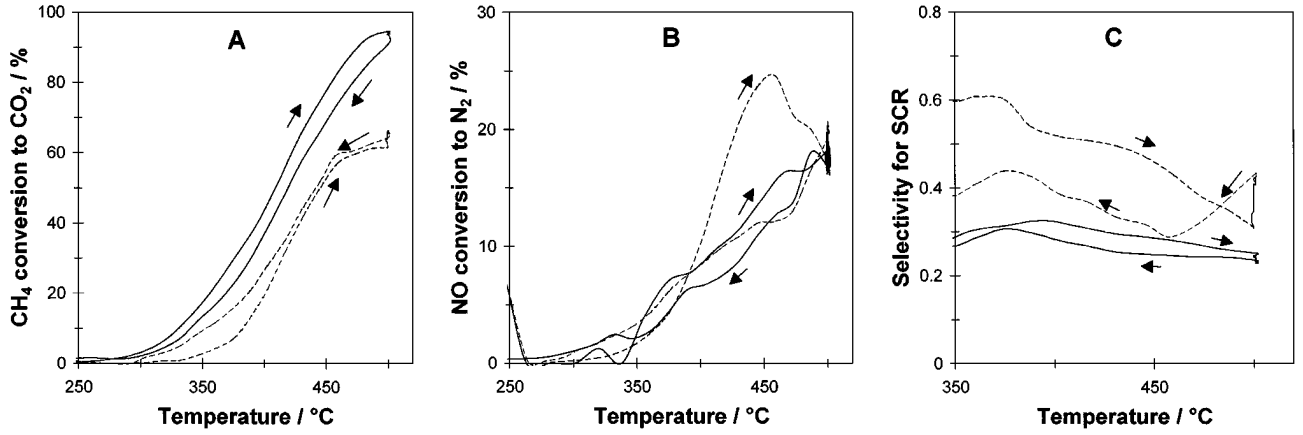

FIG. 4. Reaction of CH_4, NO, and O_2 over Pd-H-MOR-D-W catalyst as a function of the temperature: A, CH_4 to CO_2 conversion; B, NO to N_2 conversion; C, SCR selectivity for NO reduction as defined in the text. Full lines: lean mixture (2000 vpm NO, 1000 vpm CH_4, 6240 vpm O_2 in He). Broken lines: stoichiometric mixture (2000 vpm NO, 1000 vpm CH_4, 1000 vpm O_2 in He). GHSV: 30,000 h^{-1}.

specific of the Pd-H-MOR catalysts. Owing to their small half-width at half-maximum, they must be related to well-defined $Pd(NO)_x$ complexes with $x = 2$ or 3. The band at 1843 cm^{-1} (type C) is also attributed to NO adsorbed on Pd sites. Its broadness (HWHM = 44 cm^{-1}) suggests multiple Pd^{x+} sites, possibly coordinatively unsaturated Pd^{x+} sites at the surface of PdO small aggregates or particles. It must be kept in mind that all the studied mordenite samples contain large PdO particles. Hoost *et al*. have reported that the adsorption of NO on PdO supported on alumina gives rise to broad absorption in the 1900–1700 cm^{-1} region (37). Two additional bands of very weak intensity, a shoulder at ca 1780 cm^{-1} and a very broad band between 1700 and 1600 cm^{-1} can also be observed. The former is not attributed while the latter could be possibly related to nitrate/nitrite groups resulting from the reaction of NO_x with the zeolite surface (27) and/or adsorbed water. These two bands have been neglected in the curve fitting. It must be pointed out that the same four lines with about the same parameters were required for fitting all the spectra of adsorbed NO on our Pd-exchanged mordenite samples, whatever the treatment preceding the adsorption was (vide infra).

The influence of the NO adsorption temperature was evaluated by subsequently heating the sample in 0.4 Torr NO at 100, 150, and 200°C. The IR spectra were recorded at room temperature after each heating step and deconvoluted. A quantitative evaluation of the variation of integrated intensity of the four different lines as a function of heating temperature in NO is reported in Fig. 6. Clearly, the intensity of the A band significantly increased upon heating up to 100°C and remained constant upon further heating. Simultaneously the intensity of the doublet (B1 and B2

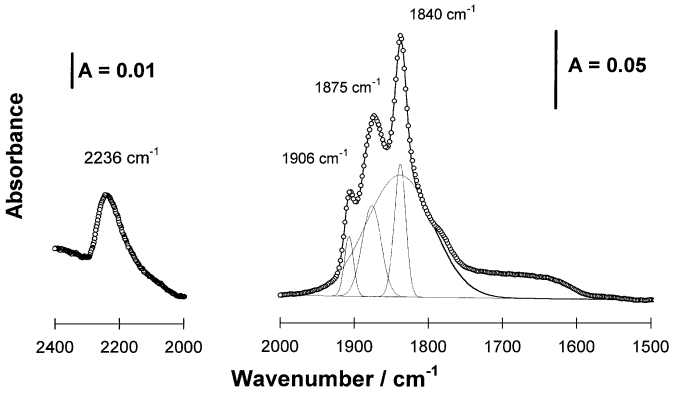

FIG. 5. FTIR spectrum of NO adsorbed at room temperature onto the Pd-H-MOR sample (NO pressure = 0.02 Torr). Experimental (○) and fitted spectra (———).

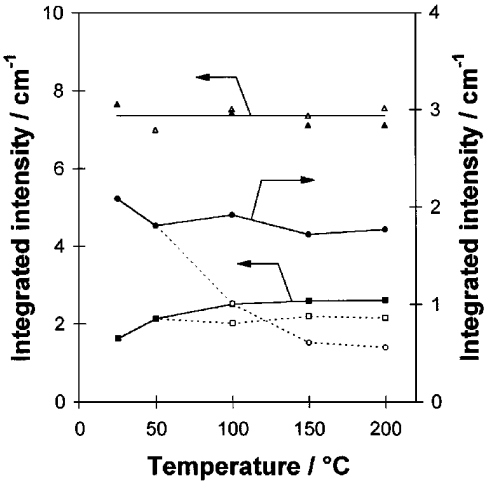

FIG. 6. Adsorption of NO onto the Pd-H-MOR sample as a function of the temperature: integrated intensities of the A, B, and C type bands (NO pressure = 0.02 Torr). Full symbols: spectra recorded at room temperature; open symbols: spectra recorded at the temperature of adsorption; (■, ❑) Type A band (1878 cm^{-1}); (●, ○) Type B (B1 + B2) band (1908 + 1839 cm^{-1}); (▲, ▽) Type C band (1843 cm^{-1}).

bands) slightly decreased while the broad C band was not affected. It is deduced that the formation of Pd mononitrosyl complexes is favored by increasing the temperature of NO adsorption.

The spectra were also recorded *in situ* at 100, 150, and 200°C in order to evaluate the strength of the Pd–NO bond of the various nitrosyl species. The integrated intensity of the various bands is compared to that obtained at room temperature after the same heating step in Fig. 6. Taking into account the uncertainty of the curve fitting, no significant variation of intensity of the types A and C bands is observed following heating and subsequent cooling down to room temperature. On the contrary, the intensity of the doublet (B1 + B2 bands) progressively decreases with increasing temperatures, compared to the intensity measured at room temperature. This points to the lower thermal stability of the species at the origin of the B1 and B2 bands, compared to Pd mononitrosyl complexes and to NO adsorbed onto Pd or PdO particles.

After evacuation at 250°C, a broad band is observed and can be resolved into a band at 1880 cm^{-1} (type A, HWHM = 15 cm^{-1}) and a broad line at 1846 cm^{-1} (type C, HWHM = 46 cm^{-1}) with the same relative intensities as before evacuation. Pd dinitrosyl complexes have been totally decomposed as expected from their low thermal stability and the remaining adsorbed NO species are removed in the same proportions. The integrated intensity of the νNO bands after evacuation at 250°C represents 25% of the intensity of the massif before evacuation, which indicates that most of the adsorbed NO has been removed from the sample. The sample was then contacted again with 0.02 Torr NO at 30°C. The spectra were recorded at increasing times and an expanded view in the 2000–1700 cm^{-1} region is shown in Fig. 7A. Immediately after contact with NO, the spectrum is dominated by the sharp intense doublet (type B bands) characteristic of the $Pd(NO)_x$ ($x = 2$ or 3) complexes while the type A band forms with a smaller intensity. Increasing adsorption time causes a decrease of the doublet and the simultaneous increase of the type A band. Two invariant points can be observed where all the curves cross perfectly. An isosbestic point is characteristic of a system where only two species are present and involved in a stoichiometric interconversion process. Considering that the 1908 and 1840 cm^{-1} bands characterize the same $Pd(NO)_x$ ($x = 2$ or 3) species, two isosbestic points are expected as observed experimentally, characteristic of the interconversion process between $Pd(NO)_x$ ($x = 2$ or 3) species and Pd mononitrosyl species.

The spectra shown in Fig. 7A were all resolved into four distinct gaussian lines as indicated above. The integrated intensities of these bands are reported in Fig. 7B as a function of the adsorption time. It will be assumed that the extinction coefficient of NO adsorbed in the various complexes is the same. Clearly the intensity of type C νNO band does not vary with adsorption time. It can be also observed that the mononitrosyl Pd species (type A νNO band) forms exactly at the expense of the $Pd(NO)_x$ ones (B1 + B2 intensities). These two plots can be fitted with an excellent agreement by log functions of the type $A_A \log(\text{time}) + K_A$ and $-A_B \log(\text{time}) + K_B$. Since the interconversion process between the two nitrosyl Pd complexes can be written as

$$Pd(NO)_x \mapsto Pd(NO) + (x-1)NO$$

with $x = 2$ or 3, by deriving the two previous functions the rate of appearance of the A band (A_A/time) and disappearance of the B bands (A_B/time) can be obtained. A ratio of A_B/A_A equal to 1.8 was found supporting the

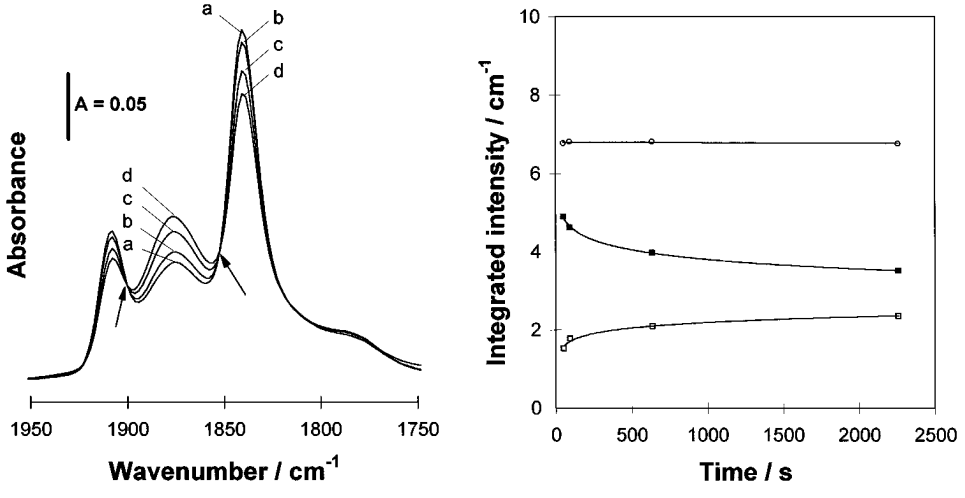

FIG. 7. Adsorption of NO at room temperature onto the Pd-H-MOR sample: A, FTIR spectra. NO (pressure = 0.4 Torr) was first adsorbed at 200°C, then evacuated at 250°C. NO was subsequently adsorbed at room temperature (P = 0.02 Torr) and spectra were recorded as a function of time after 50 s (a), 90 s (b), 640 s (c), and 2260 s (d). The arrows indicate the invariant or isosbestic points. B, Evolution with time of the integrated intensities of the A, B, and C type bands: ❑, Type A band (1878 cm^{-1}); ■, Type B (B1 + B2) band (1908 + 1839 cm^{-1}); ❍, Type C band (1843 cm^{-1}).

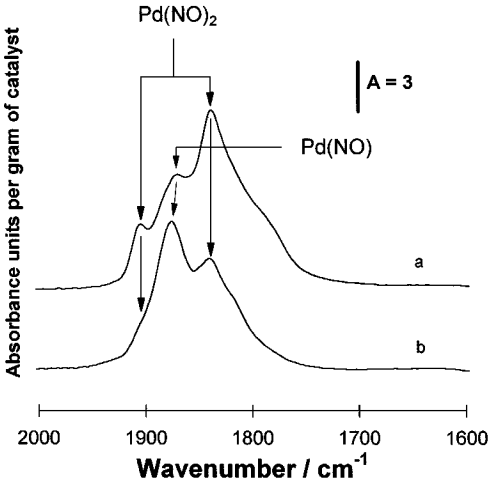

FIG. 8. FTIR spectra of NO adsorbed at room temperature onto the Pd-H-MOR-sample (a) and Pd-H-MOR-D-W (b) sample under a NO pressure of 0.02 Torr.

hypothesis of an interconversion process between mono- and di-nitrosyl Pd complexes. The $NO_2^{\delta+}$ species are simultaneously observed to slightly increase with adsorption time but this variation does not correlate with the formation of the mononitrosyl Pd complexes.

4.2. Adsorption on Pd-H-MOR-D-W. The IR spectrum in the 2000–1600 cm^{-1} region obtained upon 0.02 Torr NO adsorption at 30°C on Pd-H-MOR-D-W activated in O_2 and evacuated at 500°C is shown in Fig. 8b. It is dominated by the band (type A) at ca 1875 cm^{-1} while the doublet (type B bands) at ca 1908–1840 cm^{-1} has a much smaller intensity than for Pd-H-MOR (Fig. 8a). It can be deduced that dealumination strongly inhibits the formation of Pd dinitrosyl complexes while favoring the formation of mononitrosyl species. As a result, the integrated intensity of the A type band is 30% higher on Pd-H-MOR-D-W ($16.3 \times 10^3\,cm^{-1}\,g^{-1}$ Pd) than on Pd-H-MOR ($12.7 \times 10^3\,cm^{-1}\,g^{-1}$ Pd). The appearance of bands due to adsorbed NO is accompanied by the band at 2236 cm^{-1} related to adsorbed NO_2 as for Pd-H-MOR.

DISCUSSION

1. NO Species Adsorbed on Pd-H-MOR

From the above IR results of NO adsorption on Pd-exchanged mordenites, three distinct Pd nitrosyl species have been identified by their νNO vibrations (type A at ca 1878 cm^{-1}, type B at ca 1908 and 1839 cm^{-1}, and type C at ca 1843 cm^{-1}). Two of them form also in the Pd-H-ZSM-5 catalysts, namely the species related to the 1880 and 1840 cm^{-1} bands. The 1880 cm^{-1} band (type A) was related to a Pd mononitrosyl complex anchored to the zeolite framework and sitting as isolated species in the channels of the zeolite by analogy with the results obtained on Pd-H-ZSM-5 catalysts (27, 34). The 1840 cm^{-1} band, although still present with Pd-H-ZSM-5, has a much smaller intensity than on our Pd-H-MOR catalysts. This could be due to a higher dispersion of Pd in Pd-H-ZSM-5 catalysts because of a lower Pd loading. It was recently shown that increasing the Pd loading beyond 0.5 wt% Pd favors the formation of large PdO particles on the outer surface of ZSM-5 crystallites in addition to isolated Pd ions dispersed in the zeolite channels (34). All our Pd-H-MOR samples exhibit a significant amount of large Pd/PdO particles detected by electron microscopy. This strongly supports the attribution of the 1840 cm^{-1} band to NO adsorbed on Pd/PdO particles.

The formation of dinitrosyl Pd complexes is specific of the mordenite structure. These complexes are characterized by two νNO sharp vibrations (type B) at 1908 and 1839 cm^{-1}, corresponding respectively to the symmetric and antisymmetric vibrations associated to Pd complex in a C_{2v} symmetry. As for the gem dicarbonyl complexes, the relative intensity of the two bands is related to the angle (θ) between the two N-O oscillators (38):

$$I_{1908}/I_{1839} = [\mathrm{cotan}(\theta/2)]^2.$$

An invariant ratio of the doublet peaks is found in our experiment of NO readsorption on Pd-H-MOR evacuated at 250°C after NO adsorption. Its value of 0.43 corresponds to a NO–Pd–NO angle of 113°. This value is comparable to ones obtained with other dinitrosyl species reported in the literature: 123° on Co-Y (39), 103° on Cu-ZSM-5 (40).

The question arises to explain the formation of stable dinitrosyl Pd complexes in the mordenite structure and the interconversion process between these complexes and the Pd mononitrosyl complexes. A possible explanation might originate in the pore structure of the mordenite, made of main parallel elliptical channels (0.65 × 0.70 nm) and an interconnecting array of smaller channels, so-called *side pockets*, presenting a restricted aperture of about 0.28 nm in diameter (41, 42).

Accordingly, Pd^{2+} ions might occupy the main channels and side pockets. Upon NO adsorption, the former are expected to form Pd mononitrosyl complexes with a structure similar to that obtained in the straight channels of the H-ZSM-5 while the latter sites would be responsible for the formation of dinitrosyl complexes (not formed in H-ZSM-5 for which no such sites exist). The distribution of the Pd^{2+} cations between side pockets and main channels depends, of course, on the repartition of aluminum between these two types of sites. For a dealuminated MOR matrix, the formation of Pd dinitrosyl complexes is strongly inhibited. A first hypothesis could be that dealumination induces a preferential extraction of aluminum atoms responsible for exchange sites in side pockets. Another explanation would be the blockage of these sites by EFAL species not removed upon leaching treatments. This would explain why the Pd-H-MOR-D-W sample exhibits almost no formation of Pd dinitrosyl complexes.

The Pd dinitrosyl complexes, because of their localization in the small cavities, are expected to be coordinatively saturated with the surrounding lattice oxygen atoms acting as ligands. The conversion process of the dinitrosyl complexes into mononitrosyl complexes under NO at room temperature requires the substitution of the lattice oxygen ligands by NO, NO_2, or H_2O, allowing their migration towards large channels and their subsequent stabilization as mononitrosyl complexes.

2. *Relationship between Pd Sites and Catalytic Behavior of Pd-H-MOR Catalysts*

Pd-exchanged H-ZSM-5 catalysts have been shown to be highly active to convert NO_x into N_2 in the presence of O_2 (24–31, 34, 43, 44). At least two reactions are supposed to compete according to the following scheme:

$$CH_4 + 2\,NO + O_2 \rightarrow CO_2 + N_2 + 2\,H_2O \qquad [1]$$

$$CH_4 + 2\,O_2 \rightarrow CO_2 + 2\,H_2O. \qquad [2]$$

Reaction [1] corresponds to the reduction of NO by methane, it involves O_2 as reactant since NO_2 is suggested as a reaction intermediate and since oxygen has a promoting effect on the NO reduction. Reaction [2] corresponds to the direct combustion of methane by O_2. Very different catalytic properties have been observed, depending on the Pd loading (28, 34). At low Pd loading, reaction [1] (NO reduction) is favored and the reaction temperature has little influence on the selectivity for NO reduction. Conversely, higher Pd loading induces the increase of the selectivity for reaction [2] (methane combustion). Moreover, increasing reaction temperatures favor the combustion reaction. This behavior was attributed to the presence of PdO particles located on the outer surface of zeolite crystals. The high selectivity of the catalyst towards NO reduction in the presence of excess O_2 was attributed to the catalytic property of isolated Pd ions and/or complexes anchored to the zeolite framework and located inside the zeolite channels. The O_2 concentration has no effect on the catalytic activity of Pd ions.

Our Pd-exchanged mordenite samples do contain both PdO particles and isolated Pd^{2+} ions; the presence of large PdO particles is confirmed by electron microscopy. The increasing proportion of Pd as PdO particles should reveal the catalytic properties of bulk PdO: (i) lower selectivity for NO SCR; (ii) dependence of the selectivity for NO SCR with temperature, the combustion being favored at increasing temperatures; (iii) the combustion being more favored under lean conditions, compared to stoichiometric mixture; (iv) the formation of N_2O in the 300–450°C range. Accordingly the catalytic properties of our Pd-exchanged mordenite samples reflect the proportion of Pd as isolated cations and PdO particles. This might be dependent on several factors such as the Pd loading, the acidic properties of the zeolitic support or the activation conditions of the catalyst. The latter factor might explain the changes of catalytic behavior observed for the non-dealuminated Pd-H-MOR catalyst during the first reaction cycle (stoichiometric mixture). The activity both in NO and CH_4 conversions increases with time on stream at 500°C (Figs. 1A and B). The changes in SCR values show that the NO reduction is favored, which indicates an increase in the number of catalytic sites responsible for SCR, i.e. isolated Pd ions. This would suggest the partial redispersion of PdO particles under reactants, in accordance with recent works (43–44). X-ray absorption experiments on supported Pd catalysts have shown that the metallic Pd particles initially present on acidic supports (H-ZSM-5, H-MOR, or sulfated zirconia) are rapidly transformed into Pd^{2+} ions under a $CH_4 + NO + O_2$ mixture (43). The reaction would be assisted by the protonic acidity of the support. Of course, this mechanism could apply only to the PdO particles of small size and dispersed inside the pores of our Pd-H-MOR catalyst, the large particles observed on the outer mordenite surface remaining intact. It must be mentioned that no such changes are observed during the second cycle (lean cycle), which indicates that the catalyst has been stabilized during the stoichiometric cycle. The observed decrease of the selectivity for SCR upon changing from stoichiometric to lean conditions is indicative of the Pd^{2+}/PdO ratio, PdO particles being responsible for CH_4 combustion activity in oxygen-rich mixtures.

The hypothesis that PdO particles are redispersed into Pd ions under reactant is, however, contradicting our results obtained over Pd-H-ZSM-5 catalysts (34). We have shown that there exists a relationship between the Pd loading, the Si/Al ratio of the H-ZSM-5, and the Pd dispersion: the higher the Pd loading the lower the Pd dispersion. For Pd loading exceeding 0.5 wt% Pd, large particles are observed by electron microscopy and the selectivity of the catalyst for SCR is strongly reduced. Moreover, the activity for NO reduction decreases with time on stream at temperatures above 500°C, which suggests the transformation of isolated Pd ions (responsible for SCR) into PdO particles favoring the methane combustion. It would be expected upon these results that, owing to its high Pd loading (1 wt%), the Pd-H-MOR would exhibit a deactivation with time on stream similar to that of the Pd-H-ZSM-5 catalysts. Surprisingly, an increase of the activity is observed. An alternative explanation to the change in the catalytic behavior of the Pd-H-MOR catalyst under reactants might be given by the interconversion process between mono- and di-nitrosyl species evidenced by our IR results. The Pd^{2+} ions dispersed in the mordenite structure might occupy two different sites and form two different interconverting nitrosyl complexes upon reaction with NO while only one type of Pd nitrosyl complex (mononitrosyl species) forms in the

H-ZSM-5 structure. The latter species, related to the reaction of NO with isolated Pd ions dispersed in the zeolite (26–27), was thought to be responsible for the high activity and selectivity of Pd-H-ZSM-5 catalysts for SCR in the presence of O_2. It might be assumed that the dinitrosyl species, ascribed to species sitting in the side pockets of the mordenite structure, are inactive for SCR, the side pockets being less accessible to reactants than main channels. This hypothesis is confirmed by catalytic activity results obtained in the presence of water. It is shown that the non-dealuminated Pd-H-MOR catalyst exhibits an enhancement of its catalytic activity for SCR under wet conditions, while the addition of water to the feed generally induces a severe decrease of the catalytic activity for Pd catalysts supported on other supports, even though this decrease is somewhat limited in the case of Pd-H-ZSM-5, compared to most of the catalysts (25, 33). The loss of activity could be explained by a competitive adsorption of water on the active site. The surprising catalytic behavior of Pd-H-MOR in the presence of water can be rationalized by considering that the interconversion process between di- and mono-nitrosyl Pd species is dependent upon the amount of water in the feed. Water would be acting as a substituting ligand of the dinitrosyl complex, favoring the migration of this complex toward main channels and therefore the formation of mononitrosyl complexes, inducing the increase of the catalytic activity.

Pd in dealuminated mordenite. The Pd-H-MOR-D-W (dealuminated) sample does contain PdO particles as evidenced by transmission electron microscopy. After activation under reactants at 500°C under stoichiometric conditions, the SCR selectivity measured during the decrease in temperature from 500 to 350°C was found between 0.3 and 0.4 for the dealuminated sample instead of 0.4–0.6 for the non-dealuminated one in the same conditions (Figs. 1C and 4C). Such smaller SCR values suggest that the dealuminated catalyst exhibits larger amounts of palladium oxide in the form of big particles. It has been proposed for Pd-H-ZSM-5 catalysts that protons allow the redispersion of palladium oxide particles into isolated Pd^{x+} ions (43). For dealuminated samples, the relative number of protons compared to the number of palladium atoms is not high enough to limit the growth of the PdO particles outside of the zeolite crystallites.

Nevertheless, the conversion of NO into N_2 is higher in the case of the dealuminated sample compared to the non-dealuminated one. Such behavior is certainly due to the larger number of A species (mononitrosyl complexes) found in the Pd-H-MOR-D-W solid.

It seems there is a compensating effect between the total number of Pd^{2+} ions and the distribution between the mono and dinitrosyl species; the mononitrosyl species is favored in the case of the dealuminated sample.

CONCLUDING REMARKS

The IR study of NO adsorption on Pd exchanged mordenite catalysts calcined in O_2 at 500°C has revealed the existence of three distinct states of adsorbed NO, characterized by distinct νNO vibrations:

(i) Pd mononitrosyl complexes vibrating at ca 1880 cm^{-1}, also observed in MFI structures and thought to be responsible for the catalytic activity in NO reduction in the presence of excess O_2; these complexes could be anchored to the framework and sit in the main channels of the mordenite;

(ii) Pd dinitrosyl complexes characterized by a sharp doublet at 1908–1839 cm^{-1} and suggested to be inactive in the catalytic reaction;

(iii) NO adsorbed on Pd/PdO particles characterized by a broad νNO band centered at ca 1840–1850 cm^{-1} and thought to be active in NO reduction but less selective than isolated Pd mononitrosyl species.

The specific formation of dinitrosyl species in the mordenite structure is related to the presence of small cavities with restricted aperture, which could stabilize Pd cations but would not allow the reactants to penetrate. A stoichiometric interconversion process between mono- and dinitrosyl species was clearly shown. This process is thought to be responsible for the specific catalytic behavior of Pd mordenite catalyst in wet conditions; the activity is enhanced by addition of water to the feed.

Dealumination of the zeolite structure was shown to favor the formation of the mononitrosyl species at the expense of the dinitrosyl complexes and leads to an increase of NO SCR selectivity under stoichiometric conditions.

REFERENCES

1. Shelef, M., *Chem. Rev.* **95**, 209 (1995).
2. Armor, J. N., *Catal. Today* **26**, 147 (1995).
3. Burch, R., and Millington, P. J., *Catal. Today* **26**, 185 (1995).
4. Li, Y., and Armor, J. N., *Appl. Catal. B* **1**, L31 (1992).
5. Li, Y., and Armor, J. N., *Appl. Catal. B* **2**, 239 (1993).
6. Li, Y., and Armor, J. N., *Appl. Catal. B* **3**, L1 (1993).
7. Li, Y., Battavio, P. J., and Armor, J. N., *J. Catal.* **142**, 561 (1993).
8. Witzel, F., Sill, G. A., and Hall, W. K., *J. Catal.* **149**, 229 (1994).
9. Li, Y., and Armor, J. N., *J. Catal.* **150**, 376 (1994).
10. Li, Y., Slager, T. L., and Armor, J. N., *J. Catal.* **150**, 388 (1994).
11. Cowan, A. D., Dümpelmann, R., and Cant, N. W., *J. Catal.* **151**, 356 (1995).
12. Adelman, B. J., Beutel, T., Lei, G.-D., and Sachtler, W. M. H., *J. Catal.* **158**, 327 (1996).
13. Lukyanov, D. B., d'Itri, J. L., Sill, G., and Hall, W. K., *in* "11th International Congress on Catalysis—40th Anniversary," Studies in Surface Science and Catalysis, Vol. 101 (J. W. Hightower, W. N. Delgass, and A. T. Bell, Eds.), p. 651. Elsevier, Amsterdam, 1996.
14. Ogura, M., and Kikuchi, E., *in* "11th International Congress on Catalysis—40th Anniversary," Studies in Surface Science and Catalysis, Vol. 101 (J. W. Hightower, W. N. Delgass, and A. T. Bell, Eds.), p. 671. Elsevier, Amsterdam, 1996.

15. Aylor, A. W., Lobree, L. J., Reimer, J. A., and Bell, A. T., *in* "11th International Congress on Catalysis—40th Anniversary," Studies in Surface Science and Catalysis, Vol. 101 (J. W. Hightower, W. N. Delgass, and A. T. Bell, Eds.), p. 661. Elsevier, Amsterdam, 1996.
16. Armor, J. N., and Farris, T. S., *Appl. Catal. B* **4**, L11 (1994).
17. Li, Y., and Armor, J. N., *Appl. Catal. B* **5**, L257 (1995).
18. Li, Y., and Armor, J. N., *J. Catal.* **145**, 1 (1994).
19. Yogo, K., Ihara, M., Terasaki, I., and Kikuchi, E., *Chem. Lett.* 229 (1993).
20. Kikuchi, E., and Yogo, K., *Catal. Today* **22**, 73 (1994).
21. Tabata, T., Kokitsu, M., and Okada, O., *Appl. Catal. B* **6**, 225 (1995).
22. Kikuchi, E., Ogura, M., Terasaki, I., and Goto, Y., *J. Catal.* **161**, 465 (1996).
23. Tabata, T., Kokitsu, M., and Okada, O., *Catal. Lett.* **25**, 393 (1994).
24. Fakche, A., Pommier, B., Garbowski, E., Primet, M., and Lécuyer, C., *French Patent Appl.* 93 08 006.
25. Descorme, C., Fakche, A., Garbowski, E., Primet, M., and Lécuyer, C., *in* "1995 International Gas Research Conference, Cannes (France), 6–9 Nov. 1995," Vol. IV, p. 505.
26. Descorme, C., Gélin, P., Primet, M., Lécuyer, C., and Saint Just, J., *in* Zeolites: A refined tool for designing catalyst, Studies in Surface Science and Catalysis, Vol. 97 (L. Bonneviot and S. Kaliaguine, Eds.), p. 287. Elsevier, Amsterdam, 1995.
27. Descorme, C., Gélin, P., Primet, M., and Lécuyer, C., *Catal. Lett.* **41**, 133 (1996).
28. Loughran, C. J., and Resasco, D. E., *Appl. Catal. B* **7**, 113, 351 (1995).
29. Uchida, H., Yamaseki, K., and Takahashi, I., 2nd Japan-EC joint workshop, JECAT'95, *Catal. Today* **29**, 99 (1996).
30. Nishizaka, Y., and Misono, M., *Chem. Lett.* 2237 (1994).
31. Descorme, C., Gélin, P., Lécuyer, C., and Primet, M., *Appl. Catal. B* **13**, 185 (1997).
32. Almanza, L. O., Ph.D. thesis, Lyon 1 University, 1993.
33. Descorme, C., Ph.D. thesis, Lyon 1 University, 1996.
34. Gélin, P., Goguet, A., Descorme, C., Lécuyer, C., and Primet, M., *in* "IVth Intern. Cong. on Catalysis and Automotive Pollution Control, April 1997, Brussels," Vol. 2, p. 197.
35. Thomas, J. M., and Klinowski, J., *Adv. Catal.* **33**, 199 (1985).
36. Aylor, A. W., Lobree, L. J., Reimer, J. A., and Bell, A. T., *J. Catal.* **172**, 453 (1997).
37. Hoost, T. E., and Laframboise, K. A., *J. Catal.* **155**, 303 (1995).
38. Cotton, F. A., and Wilkinson, G., "Advanced Inorg. Chemistry," IVth ed., p. 697. Wiley, New York, 1980.
39. Windhorst, K. A., and Lunsford, J. H., *J. Am. Chem. Soc.* **97**, 1407 (1975).
40. Iwamoto, M., Yahiro, H., Mizuno, N., Zhang, W. X., Mine, Y., Furukawa, N., and Kagawa, S., *J. Phys. Chem.* **96**, 9360 (1992).
41. Breck, D., "Zeolite Molecular Sieves," Wiley, New York, 1974.
42. Meier, W. M., and Olson, D. H., *Zeolites* **12**, 1 (1992).
43. Ali, A., Alvarez, W., Loughran, C. J., and Resasco, D. E., *Appl. Catal. B* **14**, 13 (1997).
44. Adelman, B. J., and Sachtler, W. M. H., *Appl. Catal. B* **14**, 1 (1997).